



available at [www.sciencedirect.com](http://www.sciencedirect.com)



journal homepage: [www.elsevier.com/locate/jhydrol](http://www.elsevier.com/locate/jhydrol)



# Regional groundwater flow paths in Trans-Pecos, Texas inferred from oxygen, hydrogen, and strontium isotopes

Matthew M. Uliana <sup>a,\*</sup>, Jay L. Banner <sup>b</sup>, John M. Sharp Jr. <sup>b</sup>

<sup>a</sup> Department of Earth and Environmental Sciences, Susquehanna University, 514 University Avenue, Selinsgrove, PA 17870, USA

<sup>b</sup> The University of Texas at Austin, Geol Science Department, 1 University Station C1100, Austin, TX 78712-0254, USA

Received 20 April 2006; received in revised form 3 October 2006; accepted 12 October 2006

## KEYWORDS

Strontium;  
Isotopes;  
Groundwater;  
Regional flow systems;  
West Texas

**Summary** Stable isotopes, radiogenic isotopes, and major ion chemistry are used to constrain flow paths in a fracture-controlled regional groundwater flow system in far west Texas. The flow system occurs in Permian and Cretaceous sedimentary rocks and Cenozoic alluvial basin fill. Samples from springs and wells in the study area were analyzed for major ions and hydrogen, oxygen, and strontium isotopes.  $\delta D$  and  $\delta^{18}O$  values fall close to the global meteoric water line, indicating that these values have not been significantly affected by evaporation or mineral–water reactions.  $\delta^{18}O$  values from samples along the regional flow path are lower by as much as 3‰ relative to local recharge values; the distribution of stable isotope values throughout the study area suggests that lower  $\delta^{18}O$  values represent recharge during cooler climatic conditions rather than latitude or altitude effects.  $^{87}Sr/^{86}Sr$  values for water samples from along the regional flow path range from 0.7093 to 0.7148, with the highest values at the upgradient end of the flow system. These values are significantly higher than expected for groundwaters dominated by dissolution of Permian and Cretaceous marine carbonates and evaporites. The high  $^{87}Sr/^{86}Sr$  values reflect dissolution of minerals of Precambrian and early Paleozoic origin in the crystalline rocks of the Carrizo and Baylor mountains and alluvial basin fill at the upgradient end of the flow system. Contours of  $^{87}Sr/^{86}Sr$  values indicate a zone of high  $^{87}Sr/^{86}Sr$  water that corresponds to the regional groundwater flow paths. Mass-balance mixing models and mineral reactions models indicate a three end-member mixing system modified by dissolution of strontium-bearing minerals in the alluvial fill at the upgradient end of the flow system.

© 2006 Elsevier B.V. All rights reserved.

\* Corresponding author. Fax: +1 570 372 2726.  
E-mail address: [uliana@susqu.edu](mailto:uliana@susqu.edu) (M.M. Uliana).

## Introduction

Perennial springs and aquifer systems in arid and semi-arid regions are frequently sourced from large-scale regional groundwater flow systems that are controlled by fractures and other geologic structures (e.g., Babiker and Gudmundson, 2004; Uliana and Sharp, 2001; Mayer and Sharp, 1998). As many arid and semi-arid regions experience increased groundwater pumping and potential reductions in recharge from expanding areas of impervious cover, it is imperative that these regional groundwater systems be understood so that water levels and spring flows are preserved. This research delineates a regional groundwater flow system in the Trans-Pecos region of Texas, USA, using a combination of ion concentrations and stable and radiogenic isotope variations to constrain flow paths and model potential fluid mixing processes.

Trans-Pecos Texas is defined as the area of Texas west of the Pecos River and north of Big Bend National Park (Fig. 1). This is a subtropical, arid climate region (Larkin and Bomar, 1983) with an average annual rainfall of 30 cm (Schuster, 1996). Surface water resources are rare; the region is almost exclusively dependent on groundwater and spring discharge to meet municipal and agricultural needs.

Usable surface water discharges from several springs in this region (Fig. 1). San Solomon and Giffin Springs are located in Reeves County, in the village of Toyahvale, at an elevation of 1024 m above sea level (ASL). Extensive groundwater pumpage for agriculture beginning after World War II caused depressed water levels, with the result that Comanche Springs in Fort Stockton at 900 m ASL ceased to flow in the 1960 s. Water levels have recovered to the point where these springs now discharge irregularly at very low rates. Phantom Lake Springs, located at the Kingston Ranch in Jeff Davis County at 1059 m ASL, ceased to flow in early 2000 and only began to flow again after heavy rains in

2004. Numerous minor springs, such as Big Aguja Springs (~1800 m ASL) and Oak Springs (~1400 m ASL), occur in the Davis Mountains to the south.

Flow and geochemical data suggest that San Solomon, Giffin, and Phantom Lake Springs respond to local precipitation events with increases in discharge and turbidity, indicating that they are fed by a local flow system (Brune, 1981). Under baseflow conditions spring discharge maintains consistent temperatures (25–26 °C) and high total dissolved solids concentrations (TDS) (~2100 ppm) that are consistent with a regional groundwater flow system. Neilson and Sharp (1985) used water balance calculations and modeling results to suggest that water is discharging from Wildhorse Flat into the Apache Mountains (Fig. 1). LaFave and Sharp (1990) used chemical analyses of spring discharge to infer that the source of water for San Solomon and Phantom Lake Springs is partially derived from a regional groundwater flow system that originates in the bolson aquifer systems around Van Horn, Texas (Fig. 1). Uliana and Sharp (2001) used historical groundwater chemistry data and geochemical modeling to delineate hydrochemical facies in the regional groundwater of Trans-Pecos. These data support the concept of a regional groundwater flow system connecting the bolson aquifer in Wildhorse Flat to the Cenozoic Pecos Alluvium aquifer of the Toyah Basin. In addition, pre-development groundwater heads (Fig. 1) (Sharp, 1989) indicate that groundwater in the Wildhorse Flat section of the Salt Basin is flowing out of the basin through the fractured limestones of the Apache Mountains towards the springs and into the Toyah Basin.

This research uses major ion concentrations and stable and radiogenic isotope variations to test the hypothesis that a regional groundwater flow system connects Wildhorse Flat with the Toyah Basin (Fig. 2). Twenty-nine water samples were taken from wells and springs in the study area (Fig. 2). All samples were analyzed for  $^{87}\text{Sr}/^{86}\text{Sr}$ ; 23 samples were analyzed for cation (Ca, Mg, Na, K, and Sr) and anion

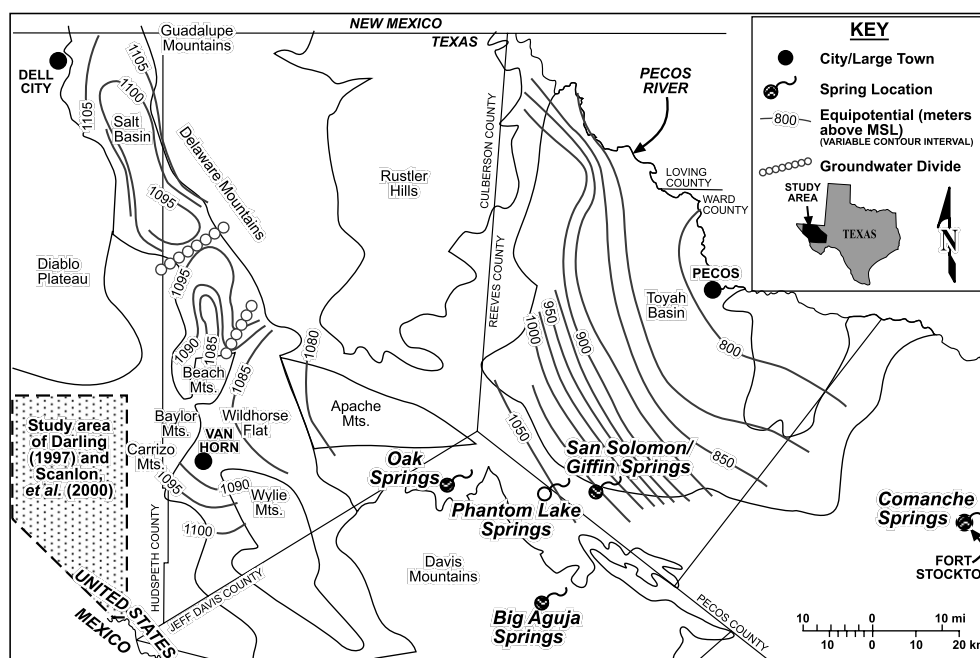


**Figure 1** Study area showing physiographic regions, county boundaries, spring locations, and pre-development groundwater heads (after Sharp, 1989).

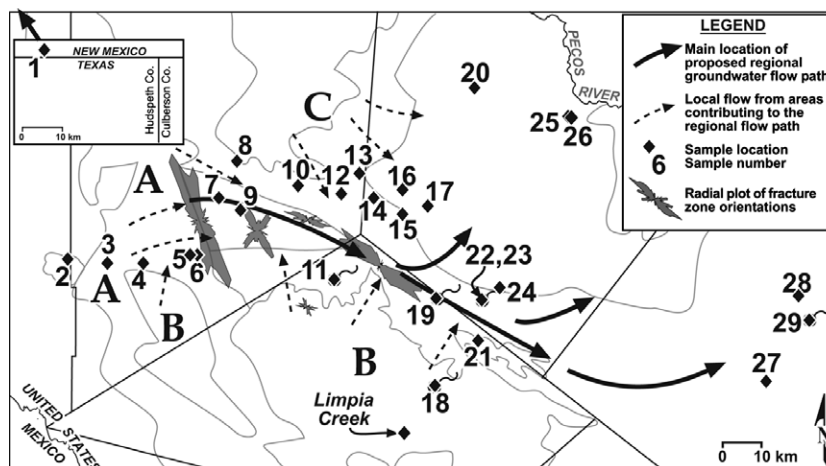


**Figure 2** Study area showing sample locations including Limpia Creek samples analyzed by Coplen and Kendall (2000). The solid arrows indicate the main location of the proposed regional flow system (Uliana and Sharp, 2001; Uliana, 2000); the dashed lines represent contributions from end-member areas A, B, and C.

( $\text{SO}_4$ , Cl,  $\text{NO}_3$ , and  $\text{HCO}_3$ ) concentrations; 19 samples were analyzed for  $\delta^{18}\text{O}$ , and 13 samples were analyzed for  $\delta\text{D}$ .

### Physiography and geology

Trans-Pecos Texas lies within the Basin and Range physiographic province. Ground elevation ranges from about 700 m ASL along the Pecos River to 2667 m ASL at Guadalupe Peak in the Guadalupe Mountains. Exposures of Precambrian metasediments and Lower Paleozoic (Cambrian to Ordovician) siliciclastic rocks occur in the Carrizo, Baylor, and Beach mountains (Fig. 1). The Apache and Guadalupe Mountains are portions of the reef that circled the Late Permian Delaware Basin. The Delaware Mountains consist of Mid- to Upper Permian (Leonardian–Guadalupian) limestones and sandstones deposited in the Delaware Basin. The Rustler Hills are primarily evaporites and carbonates (anhydrite and dolomite) deposited after the Delaware Basin was cut off from the ocean in the Late Permian. The evaporites and siliciclastic basin fill facies dip to the east and are present at depth in Reeves and Pecos counties. Lower Cretaceous limestones overlie the Permian rocks south and east of the Apache Mountains. Cretaceous rocks crop out to the south and east of the Apache Mountains along the Reeves-Jeff Davis county line and in Pecos County. The Davis Mountains consist of Eocene to Oligocene lava flows and ash-flow tuff deposits that overlie the Cretaceous system in Jeff Davis County. Cretaceous limestones in the Toyah Basin are overlain by a thick sequence of Cenozoic alluvium that is up to 470 m thick in the center of the basin (Ashworth, 1990). Tertiary and Quaternary alluvial sediments also occur in the Salt Basin graben at thickness of over 750 m (Gates et al., 1980).

Radial plots of length-weighted fracture orientations (Fig. 2) taken from pre-existing geology maps (Wood, 1965; Barnes, 1976, 1979, 1995a,b) show three significant fracture trends in the area; one at  $\sim\text{N}25\text{W}$ , one at  $\sim\text{N}40\text{E}$ , and a third between  $\text{N}55\text{W}$  and  $\text{N}70\text{W}$ . The fracture trends between the eastern part of the Apache Mountains and the main springs along the Reeves-Jeff Davis County line

are parallel to the proposed regional flow paths and suggest that fracture networks are controlling the location of the hypothesized regional flow system. Details concerning the relationship between fracture trends and groundwater flow paths in the study area, including length-weighting of fracture orientations and a lineament analysis of aerial photographs, can be found in Uliana (2000) and Sharp et al. (2000).

A detailed overview of the groundwater chemistry in the study area, including a delineation of hydrochemical facies and the use of historical data to delineate the regional flow paths discussed in this paper, is presented in Uliana and Sharp (2001).

### Analytical methods

Water samples were collected from wells and springs. Spring waters were sampled as close to the spring orifice as possible. Wells were pumped for a minimum of 5 min before sampling, specific conductivity and pH of the discharge water were monitored, and sample bottles were filled after these parameters stabilized. All deep wells were active at the time of sampling, so the samplers have a high degree of confidence that the water samples represent the formations. Sample bottles were kept in a cooler or refrigerator upon collection.

Cation analyses were performed using a Perkin-Elmer/Sciex Elan 5000 ICP-MS in the University of Minnesota or using a JY ICP-OES in the Department of Geological Sciences at The University of Texas at Austin. Anion analyses were performed by ion chromatography at the Department of Geological Sciences at The University of Texas at Austin. Random duplicates of all cation and anion analyses were within 5%, and field and laboratory blanks were below detection limits for all species. Charge balances for all samples with  $\text{HCO}_3$  data are less than 5%.

Hydrogen ( $\delta\text{D}$ ) and oxygen ( $\delta^{18}\text{O}$ ) isotope analyses were performed on a VG SIRA 12 and a VG Prism gas source mass spectrometer, respectively, in the Department of Geological Sciences at The University of Texas at Austin. Analytical

precision for  $\delta D$  and  $\delta^{18}O$  values of waters is  $\pm 1\text{‰}$  and  $\pm 0.1\text{‰}$ , respectively. Analytical methods for  $\delta^{18}O$  are given in Mickler et al. (2004). Analytical methods for  $\delta D$  are described in Coleman et al. (1982) and Kendall and Coplen (1985), with the exception of "Indiana zinc" turnings substituted for the zinc shot specified in those references.

Water samples for  $^{87}Sr/^{86}Sr$  analyses were collected in acid-cleaned bottles; an aliquot was then dispensed in the lab to Teflon vials and evaporated to dryness on a hotplate. Samples were dissolved in 330  $\mu L$  of 0.3 M ultra-pure  $HNO_3$  for ion exchange chemistry. Sr was separated via cation exchange using 120  $\mu L$  Teflon micro-columns, Eichrome Industries Inc. Sr Specific resin (fine), ultra-pure  $HNO_3$ , and nanopure deionized water.

Strontium isotope analyses ( $^{87}Sr/^{86}Sr$ ) were conducted in the Department of Geological Sciences at The University of Texas at Austin on a Finnigan-MAT 261 thermal ionization mass spectrometer. Procedures followed those of Banner and Kaufman (1994). Approximately 200 nanograms of Sr were loaded onto single rhenium filaments in dilute  $HNO_3$  with a  $H_3PO_4 + Ta_2O_5$  slurry loading medium. All analyses were determined in dynamic multicollection mode.  $^{87}Sr/^{86}Sr$  values were normalized for fractionation to an  $^{87}Sr/^{86}Sr$  value of 0.1194 using an exponential fractionation law, and were also corrected offline for fractionation using an in-house correction based on an empirical relationship

between instrument fractionation and  $^{87}Sr/^{86}Sr$  value. During the study period the NIST SRM 987 standard was analyzed 85 times with a mean  $^{87}Sr/^{86}Sr$  of 0.710265 and an external  $2\sigma$  of 0.000018. Each isotopic ratio represents an average of 60 to 105 individual ratios (4–7 blocks of 15 scans per block). Laboratory blank values for Sr were less than 80 pg and are negligible with respect to the  $\sim 200$  ng quantities of sample analyzed.

## Results

Analytical results are presented in Table 1. Nineteen samples were analyzed for  $\delta^{18}O$ , and thirteen samples were also analyzed for  $\delta D$ .  $\delta^{18}O$  values range from  $-9.2\text{‰}$  to  $-6.8\text{‰}$ .  $\delta D$  values range from  $-66\text{‰}$  to  $-48\text{‰}$ .  $\delta^{18}O$  and  $\delta D$  values for all samples lie close to the global meteoric water line (Fig. 3). Samples from Big Aguja Springs (sample 18), located in the Davis Mountains at an elevation of 1800 m ASL; from a well at the northeastern edge of the Davis Mountains (sample 21); and from a well at the southern end of the Rustler Hills (sample 10), have  $\delta^{18}O$  values of  $-7.0\text{‰}$ ,  $-7.1\text{‰}$ , and  $-6.8\text{‰}$ , respectively (Fig. 4). The samples located along the hypothesized regional flow path have  $\delta^{18}O$  values that range from  $-9.2\text{‰}$  to  $-7.7\text{‰}$ .

Twenty-nine water samples were analyzed for  $^{87}Sr/^{86}Sr$ .  $^{87}Sr/^{86}Sr$  values range from 0.7074 to 0.7148. Seventeen of

**Table 1** Analytical results

ID#	Sample location	$^{87}Sr/^{86}Sr$	$\delta^{18}O$	$\delta D$	Ca	Mg	Na	K	Sr	SO <sub>4</sub>	Cl	NO <sub>3</sub>	HCO <sub>3</sub>
1	Duggar Well	0.708016			208	64.3	16	1.4	4.5	521	12	3.9	317
2	Koehn Ranch Well	0.714797											
3	Van Horn City Well	0.712659	-7.7	-54	20.4	8.7	121	7.3	0.36	77	47	9.9	261
4	Koehn House Well	0.707885			16.3	3.12	69	12	0.20	28	29	4.9	
5	Plateau Old Well	0.710822	-8.2	-57	144	64	404	21	2.4	492	541	6.2	270
6	Plateau New Well	0.710814			157	78.1	423	38	3.0	532	651	0.62	277
7	Apache Ranch Well 3	0.710111	-9.2	-66	145	75.3	325	99	2.4	681	685	0.13	
8	Clayton Well	0.709188			203	74	307	95	2.6	882	644	4.0	
9	Apache Ranch Deep Well	0.710343	-8.7	-60	68	37.3	100	67	0.68	191	181	0.71	
10	Foster Ranch House Well	0.708012	-6.8	-48	471	61.5	71	69	2.9	1498	54	33	
11	Oak Springs	0.708175			24.6	2.34	13	10	0.15	6.2	3.8	1.2	
12	Far West Well	0.708577	-8.3	-56	237	70.8	197	51	3.1	798	343	1.3	
13	Axtel Well	0.708512			304	96.6	127	63	4.6	1108	238		
14	Bull Mill Well	0.708176			371	91.6	249	41	4.9	1304	431	0.14	
15	F-M Well S 28	0.708871	-8.3	-55									
16	Middle Well	0.708160			443	110	324	31	6.1	1546	547		
17	F-M Well 4	0.707962	-8.5	-58	92	19	77			211	61	33	178
18	Big Aguja Springs	0.707609	-7.0	-48	42.0	5.2	22	3.7	0.22	7.3	6.9	1.2	197
19	Phantom Lake Springs	0.710007	-9.0	-61	183	83.1	453	22	3.6	650	619		321
20	Irrigation Well	0.708733	-7.3										
21	Catfish Pond Well	0.707754	-7.1										
22	San Solomon Springs	0.709991	-8.7	-62	177	77.8	420	20	3.3	621	587		275
23	Giffin Spring	0.709999	-8.7										
24	West Sandia	0.709683	-7.9										
25	TAMU Ag Station #2	0.708262	-8.1	-57	160	47.1	759	11	3.1	901	799	20	237
26	TAMU Ag Station #3	0.708373			43.0	11.2	744	5.8	0.91	808	459		353
27	Belding Irrigation Well	0.709725	-7.8		156	65.6	289	13	3.1	475	404	6.7	292
28	Rustler Well	0.707445	-7.8		582	200	214	14	10.2	212	282		185
29	Comanche Springs	0.709265	-7.5	-51	256	113	358	15	5.8	881	512	23.2	322

$\delta^{18}O$  and  $\delta D$  are in ‰ SMOW. All cation and anion concentrations are in ppm.

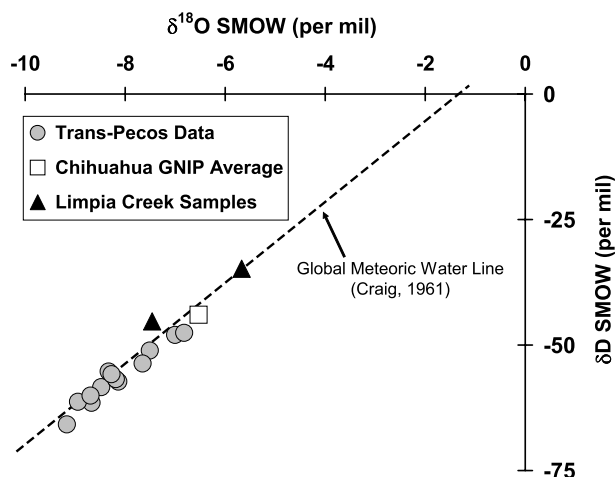


**Figure 3**  $\delta^{18}\text{O}$  versus  $\delta\text{D}$  values in groundwaters of this study area compared to the global meteoric water line (Craig, 1961). The open square is the annual weighted mean for the Global Network of Isotopes in Precipitation (GNIP) station at Chihuahua, Mexico.

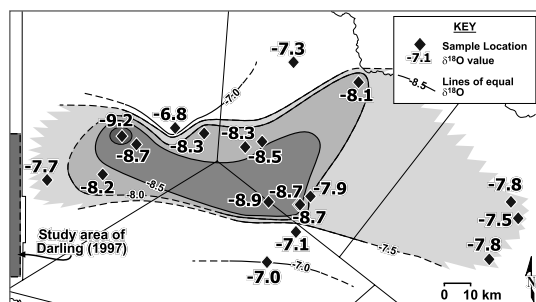


**Figure 4**  $\delta^{18}\text{O}$  values in groundwater and spring samples throughout the study area. The shaded areas delineate samples with  $\delta^{18}\text{O}$  values that are less than those expected for waters dominated by local meteoric recharge ( $-7.5\text{‰}$ ). Values are contoured with a  $0.5\text{‰}$  interval with darker zones representing lower  $\delta^{18}\text{O}$  values. The study area of Darling (1997), including Eagle Flat and Red Light Draw, is located between the dashed line and the Rio Grande to the west of the map area.

these samples have  $^{87}\text{Sr}/^{86}\text{Sr}$  values that are greater than or equal to 0.7085 and nine samples are greater than or equal to 0.7100 (Fig. 5). Samples taken from the Carrizo Mountains, Wildhorse Flat, the Apache Mountains, and San Solomon, Giffin, and Phantom Lake Springs have  $^{87}\text{Sr}/^{86}\text{Sr}$  values greater than 0.7100, with the highest values ( $>0.712$ ) located in and near the Carrizo Mountains. In addition, samples 8, 24, 27, and 29 have  $^{87}\text{Sr}/^{86}\text{Sr}$  values greater than 0.7090. The significance of these values in relation to the values expected from waters dominated by interaction with the Permian and Cretaceous marine sedimentary rocks, Tertiary volcanics, and Cenozoic alluvial fill are discussed in the following section.

## Discussion

In the following section we discuss the expected isotopic values, the results of our oxygen–deuterium and strontium

isotopic values, and models of chemical and isotopic evolution.

### Expected isotope values

Oxygen and hydrogen isotopes of the water molecule are indicators of conditions present at the time and place of groundwater recharge (Faure, 1986).  $\delta^{18}\text{O}$  and  $\delta\text{D}$  values are compared to the meteoric water line (MWL) of Craig (1961). Stable isotope values that plot along the MWL are compared to local precipitation values to determine if the groundwater is derived from recent local recharge or if it is derived from water that recharged under different climatic conditions. Deviations from the MWL indicate modification of the groundwater by evaporation or extensive mineral–water reactions.

$\delta^{18}\text{O}$  and  $\delta\text{D}$  values for local precipitation throughout the study area are not well documented. A general estimate, however, can be derived from data and study results from nearby areas. Data from the nearest Global Network for Isotopes in Precipitation (GNIP) station (#7622500, located in Chihuahua, Mexico at an elevation of 1423 m) have weighted mean  $\delta^{18}\text{O}$  and  $\delta\text{D}$  values of  $-6.5\text{‰}$  and  $-44\text{‰}$ , respectively (IAEA/WMO, 2001).  $\delta^{18}\text{O}$  values in precipitation from GNIP stations throughout North America were used to develop a distribution of weighted annual average  $\delta^{18}\text{O}$  values in precipitation for the United States and northern Mexico (IAEA/WMO, 2001). This distribution indicates that both the study area and the Chihuahua GNIP station fall within a region of weighted mean  $\delta^{18}\text{O}$  values ranging from  $-10$  to  $-6\text{‰}$  and that each is closer to the higher end of the range.

$\delta^{18}\text{O}$  values in precipitation in Eagle Flat, about 15 km west of Van Horn, Texas at an elevation of about 1,300 m (Fig. 1) are presented in Darling (1997) and Scanlon et al. (2000). Weighted mean  $\delta^{18}\text{O}$  values for these data are  $-6.8\text{‰}$ .

Springs and gaining streams in high altitude areas are generally recharged locally from short groundwater flow systems; thus, these samples will represent an integrated sample of precipitation from the catchment area above the sample location. Samples from two locations in the Davis Mountains – Big Aguja Springs (sample 18), which discharge at an elevation of 1800 m ASL; and Limpia Creek, sampled at an elevation of 1580 m (Coplen and Kendall, 2000) – have  $\delta^{18}\text{O}$  values that range from  $-7.5\text{‰}$  to  $-5.7\text{‰}$ . Based on the GNIP data, the results from Eagle Flat, and the Davis Mountains data, precipitation in the study area should have  $\delta^{18}\text{O}$  values ranging from  $-7.5\text{‰}$  to  $-5.7\text{‰}$ .

Strontium isotopes can trace groundwater flow paths through the regional flow system (e.g., Musgrove and Banner, 1993; Banner et al., 1994; Armstrong et al., 1998). An aspect of strontium isotopic ratios that makes them particularly useful in tracing regional groundwater flow paths and identifying mixing relationships in regional flow systems is that they undergo negligible fractionation during mineral–water reactions (i.e., mineral dissolution or precipitation, Banner and Kaufman, 1994). Groundwaters that are in equilibrium with strontium-bearing minerals are therefore expected to have  $^{87}\text{Sr}/^{86}\text{Sr}$  values that reflect the isotopic ratio of the minerals.

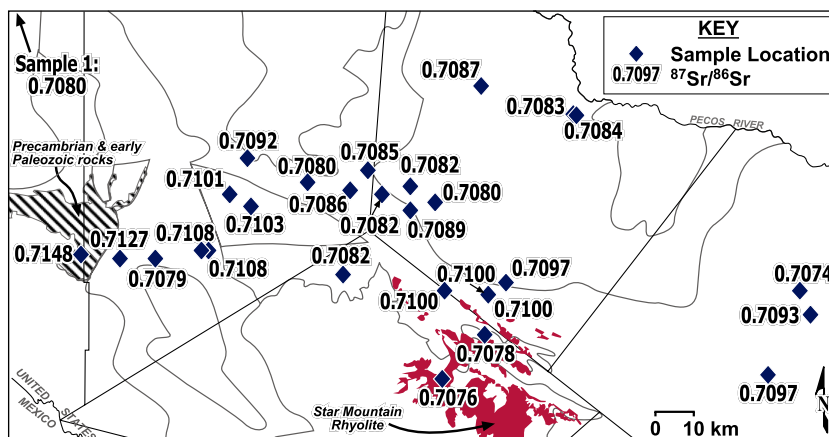


Figure 5  $^{87}\text{Sr}/^{86}\text{Sr}$  values in groundwater and spring samples throughout the study area.

$^{87}\text{Sr}/^{86}\text{Sr}$  values in feldspar separates from 21 rhyolite, basalt, and tuff samples from the Davis Mountains range from 0.7037 to 0.7275 and average 0.7067 (Cameron et al., 1996). Eighteen of these samples have  $^{87}\text{Sr}/^{86}\text{Sr}$  values less than 0.708 while the remaining three samples are greater than 0.711. The samples with  $^{87}\text{Sr}/^{86}\text{Sr}$  values greater than 0.711 are located in a felsic lava flow formation, the Star Mountain Rhyolite, that unconformably overlies Cretaceous sedimentary rocks in the eastern half of Jeff Davis County. These data suggest that water samples from the Star Mountain Rhyolite could have  $^{87}\text{Sr}/^{86}\text{Sr}$  values as high as 0.728, while samples from other parts of the Davis Mountains should have values ranging from 0.703 to 0.708.

Variations in  $^{87}\text{Sr}/^{86}\text{Sr}$  values for seawater from the Cambrian to the present as determined by Burke et al. (1982), Brookins (1988), and Denison et al. (1994) indicate that Permian or Cretaceous marine carbonates and evaporites, and sediments derived from those rocks, should have  $^{87}\text{Sr}/^{86}\text{Sr}$  values that range from 0.7068 to 0.7084. Denison et al. (1998) determined  $^{87}\text{Sr}/^{86}\text{Sr}$  values for anhydrite beds in the Late Permian (Ochoan) Rustler Formation ranging from 0.7069 to 0.7074. Permian carbonates and evaporites and Cretaceous carbonates dominate the regional groundwater system north of the Davis Mountains; here water samples are expected to have  $^{87}\text{Sr}/^{86}\text{Sr}$  values that range from 0.7068 to 0.7084.

No Sr isotope data were found in the literature for the rocks or sediments at the upgradient end of the regional flow system, including the bolson sediments in Wildhorse Flat and the rocks and alluvial sediments in the Carrizo, Baylor, and Beach mountains on the western edge of Wildhorse Flat (Fig. 1). Sr isotope values for the groundwaters in these areas are also not available in the literature. However, the mountains along the western edge of Wildhorse Flat comprise Precambrian metasediments and igneous intrusives, and Cambrian/Ordovician siliciclastics; and much of the sediments in the western part of the Wildhorse Flat bolson are derived from the Precambrian/Early Paleozoic strata. If we assume that the chemistry of the groundwaters in the Wildhorse Flat area are dominated by mineral/water interactions with these Precambrian/Early Paleozoic silicate minerals, then we would expect water samples from this area have  $^{87}\text{Sr}/^{86}\text{Sr}$  values that are significantly higher than those from the other parts of the study area.

### Oxygen and hydrogen isotope variations

When plotted against the global meteoric water line (Fig. 3), study area samples do not show patterns of enrichment that could be attributed to evaporation of meteoric water during recharge (Allison, 1982) or to extensive mineral–water interactions following recharge (Banner et al., 1989). Therefore,  $\delta^{18}\text{O}$  values in these samples likely reflect the conditions present at the time of recharge, and that evaporation and mineral–water interactions have not significantly affected the stable isotope values.

Samples from the Davis Mountains (samples 18 and 21) and from the Rustler Hills (sample 10) have  $\delta^{18}\text{O}$  values that fall within the range of local precipitation values, suggesting that these samples represent local meteoric recharge. The samples located along the hypothesized regional flow path have lower values that suggest that they are not derived from recent local precipitation. This discrepancy could be caused by ground surface altitude differences, different source areas of water vapor, differences in distance from the source area, or differences in local climate at the time and point of recharge (Faure, 1986).

Precipitation at higher altitudes has lower  $\delta^{18}\text{O}$  values, generally  $-2$ – $-3$ ‰/km (Fontes, 1980). If altitude of ground surface elevation is controlling groundwater  $\delta^{18}\text{O}$  values then the lightest values should be associated with the highest elevations. This relationship between elevation and  $\delta^{18}\text{O}$  is not observed in the study area. Well and spring samples from high elevations in the Davis Mountains (samples 18 and 21) have  $\delta^{18}\text{O}$  values that are up to 1.9‰ higher than samples from the springs located at the base of the mountains, indicating that lower  $\delta^{18}\text{O}$  values are not associated with higher ground surface elevations. This indicates that altitude is not primarily responsible for the discrepancy between the groundwater  $\delta^{18}\text{O}$  and the value of  $\delta^{18}\text{O}$  in local precipitation.

Higher latitudes are generally associated with lower  $\delta^{18}\text{O}$  values in precipitation. Continental regions of Europe and North America tend to exhibit a variation of  $\sim 0.6$ ‰ per degree latitude (Clark and Fritz, 1997). Latitudes of the sample locations in our study area range from  $30^{\circ}30'$  to  $31^{\circ}30'$ , suggesting that latitude could only account for a variation of about 0.6‰, or 25% of the total range of  $\delta^{18}\text{O}$  values measured in the study area. In addition, there is not a

direct correlation between latitude and  $\delta^{18}\text{O}$  values. Sample 20, which is the northernmost of all the  $\delta^{18}\text{O}$  samples, has a  $\delta^{18}\text{O}$  value that is consistent with the range of local precipitation values for the Davis Mountains. In addition, sample 10, which has the highest  $\delta^{18}\text{O}$  value ( $-6.8\text{‰}$ ), is located at approximately the same latitude as sample 7, which has the lowest  $\delta^{18}\text{O}$  value ( $-9.2\text{‰}$ ). These data suggest that latitude is not responsible for the lower  $\delta^{18}\text{O}$  values.

Cooler precipitation temperatures are generally associated with lower  $\delta^{18}\text{O}$  values in precipitation. Climate does not significantly vary across the study area, and the variations in climate that do occur (i.e., lower temperatures at higher elevations) are associated with  $\delta^{18}\text{O}$  values that are opposite of what would be expected (e.g., higher  $\delta^{18}\text{O}$  values occur in the Davis Mountains and lower  $\delta^{18}\text{O}$  values occur at lower elevations). However, climate in the study area was much cooler and wetter during the last glacial maximum (LGM) and the early Holocene (Hoyt, 2000). Several studies present estimated differences in mean annual ground temperature in Texas and New Mexico of  $5\text{--}8\text{ }^\circ\text{C}$  between the present and the LGM (Stute et al., 1992; Anderson, 1993; Toomey et al., 1993; Dutton, 1995; Stute et al., 1995). Dansgaard (1964) compared annual mean  $\delta^{18}\text{O}$  of precipitation to annual mean air temperature for a large number of samples and determined a  $\delta^{18}\text{O}$ -temperature relationship of  $0.69\text{‰}/^\circ\text{C}$ , while Van der Straaten and Mook (1983) determined a  $\delta^{18}\text{O}$ -temperature relationship of  $0.55\text{‰}/^\circ\text{C}$ . These temperature fractionation gradients correspond to a  $3\text{--}5\text{‰}$  depletion of  $\delta^{18}\text{O}$  in precipitation during the LGM compared to present values. Adding these depletion factors to the estimated  $\delta^{18}\text{O}$  values for recent precipitation results in  $\delta^{18}\text{O}$  values of  $-12.5\text{‰}$  to  $-8.5\text{‰}$  in precipitation during the LGM. The  $\delta^{18}\text{O}$  values of samples from locations along the main part of the regional flow path fall in the high end of this range. These are, therefore, interpreted to represent recharge during the latter Pleistocene.

Groundwater isotope values published by Darling (1997) from the Eagle Flat and Red Light Basins show a similar  $\delta^{18}\text{O}$  trend of values at the highest altitudes within the range of local precipitation ( $-7.5\text{‰}$  to  $-6\text{‰}$ ) and values from lower elevations in the basins as low as  $-10\text{‰}$  (Darling, 1997). Darling (1997) concluded that the higher altitude samples represent recent recharge, while the lower values in the basins represent water that recharged during the cooler climate of the late Pleistocene. Darling (1997) also identified a correlation between  $\delta^{18}\text{O}$  and  $^{14}\text{C}$  that indicates depleted  $\delta^{18}\text{O}$  values associated with  $^{14}\text{C}$  values of 20 pmc or less. This supports the conclusion that depleted  $\delta^{18}\text{O}$  waters represent significantly older recharge.

One other possible explanation for the observed  $\delta^{18}\text{O}$  values is that the lower  $\delta^{18}\text{O}$  values in the groundwater could be the result of the "amount effect" (Dansgaard, 1964). In areas where air temperatures exceed a certain threshold (the "amount effect threshold"; approximately  $20^\circ\text{C}$ ) and precipitation is relatively high, the values of  $\delta^{18}\text{O}$  in precipitation will decrease with increasing precipitation. In tropical regions, where the amount effect threshold is constantly exceeded,  $\delta^{18}\text{O}$  values are inversely proportional to precipitation amounts (Rosanski et al., 1993; Higgins and MacFadden, 2004). Evaluating the potential impact of the amount effect on precipitation in this area, however, is problematic

because temperatures only exceed the amount effect threshold for part of the year, and precipitation amounts are variable as well. Darling (1997) and Scanlon et al. (2000) did not specifically identify an amount effect in the Eagle Flat and Red Light Basins west of the study area. Data on monthly average oxygen isotopes, precipitation amounts, and air temperatures for the Chihuahua GNIP station (Fig. 6) are not conclusive. Precipitation and temperature indicate that an amount effect may be possible in June through September, yet a noticeable decrease in  $\delta^{18}\text{O}$  only occurs in September. Average values for the summer months represent one value per year for a 17–22 year period, so the data coverage may not be enough to adequately identify the long-term trends. At this time, we cannot rule out the amount effect as a possible influence on  $\delta^{18}\text{O}$  values. However, the consistency between our data and the results of Darling (1997), along with the spatial relationships between locations of low  $\delta^{18}\text{O}$  values and the hypothesized regional flow paths, support the interpretation of recharge during the latter Pleistocene.

### Strontium isotope variations

Sample 28, a high-TDS Ca– $\text{SO}_4$  water taken from an abandoned oil test well completed into the Permian (Ochoan) Rustler Formation at a depth of over 1000 m, has a  $^{87}\text{Sr}/^{86}\text{Sr}$  value of 0.7074 and a molar  $(\text{Ca}+\text{Mg})/(\text{HCO}_3+\text{SO}_4)$  of 0.91 (Table 1). This Sr isotope value is consistent with those expected from water dominated by dissolution of Late Permian evaporites and/or carbonates (Denison et al., 1998), and  $(\text{Ca}+\text{Mg})/(\text{HCO}_3+\text{SO}_4)$  values near unity are consistent with those expected from dissolution of evaporites and carbonates. Sample 1, from a well completed in Permian (Wolfcampian or Leonardian) limestone, has a  $^{87}\text{Sr}/^{86}\text{Sr}$  value of 0.7080 and a molar  $\text{Ca}/\text{SO}_4$  of 0.95. Sample 4, taken from a shallow, low-TDS well that most likely represents recent recharge from the Permian (Wolfcampian and Leonardian) carbonates in the Wylie Mountains, has an  $^{87}\text{Sr}/^{86}\text{Sr}$  value of 0.7079 and a molar  $\text{Ca}/\text{SO}_4$  of 1.4. These strontium isotope values and ion ratios are consistent with those expected from interaction of groundwater with Early and Middle Permian marine sediments (Brookins, 1988; Denison et al., 1994).

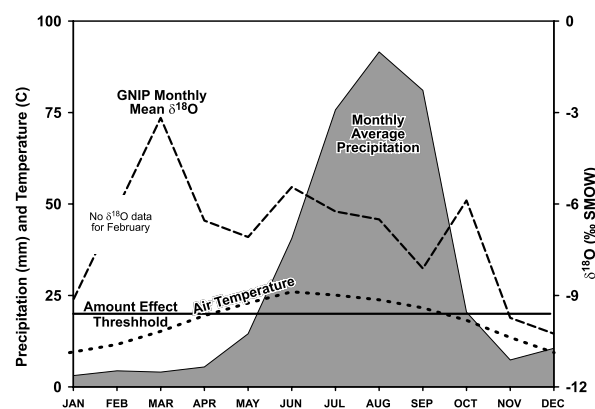


Figure 6 Monthly average  $\delta^{18}\text{O}$  in precipitation, precipitation amounts, and air temperatures at the Chihuahua GNIP station.

Samples 18 (Big Aguja Springs) and 11 (Oak Springs), located in the Davis Mountains, have  $^{87}\text{Sr}/^{86}\text{Sr}$  and molar  $\text{Ca}/\text{SO}_4$  values of 0.7076 and 13.8, and 0.7082 and 9.6, respectively. Sample 21 (Catfish Pond Well), also located in the Davis Mountains, has an  $^{87}\text{Sr}/^{86}\text{Sr}$  value of 0.7078. High  $\text{Ca}/\text{SO}_4$  ratios are consistent with waters dominated by dissolution of calcium-bearing silicate minerals such as those present in the volcanics in the Davis Mountains (Cameron et al., 1996). The Sr isotope values are also consistent with the majority of the whole-rock isotope values for the Davis Mountains volcanics also presented in Cameron et al. (1996). These ion ratios and isotope values are therefore interpreted to represent the interaction of meteoric recharge with the volcanics in the Davis Mountains.

Cameron et al. (1996) reported a small number of whole-rock isotope values for the Star Mountain Rhyolite (Fig. 6) that were greater than 0.711, suggesting that a possible source of high  $^{87}\text{Sr}/^{86}\text{Sr}$  in the groundwater is the Star Mountain Rhyolite. However, this formation is not present in the remainder of Jeff Davis County or in Culberson County (Barnes, 1979, 1995a) near the wells with the highest  $^{87}\text{Sr}/^{86}\text{Sr}$ . In addition, samples taken from a spring and a well in the Star Mountain Rhyolite (samples 18 and 21) have  $^{87}\text{Sr}/^{86}\text{Sr}$  values of 0.7076 and 0.7078, respectively. This suggests that the Star Mountain Rhyolite is not the source of high  $^{87}\text{Sr}/^{86}\text{Sr}$  in the regional flow system.

It should be noted that, while the ion ratios presented in the previous three paragraphs can be used to distinguish between the waters of the Davis Mountains and those dominated by interactions with the Permian carbonates and evaporites, the range of Sr isotope values for each of these two groups of water samples are essentially identical, so the Sr data alone cannot be used to distinguish between the two groups. However, the Sr isotope ratios for each group are consistent with the expected values for those areas based on the lithology of the hydrostratigraphic units present. Furthermore, when considered in conjunction with the ion chemistry and the geographic location of the samples, the Sr data indicate that the waters in these areas are consis-

tent with waters derived from interactions with the local mineral assemblages.

Another possibility for high  $^{87}\text{Sr}/^{86}\text{Sr}$  in the groundwater is dissolution of minerals within the Precambrian and early Paleozoic siliciclastics that occur in the Carrizo, Baylor, and Beach Mountains on the western edge of Wildhorse Flat (Fig. 5) and in the alluvial fan deposits in Wildhorse Flat that are derived from those mountains. The groundwater samples with the highest  $^{87}\text{Sr}/^{86}\text{Sr}$  values (samples 2 and 3) are associated with those formations, suggesting that groundwater interaction with the Precambrian-early Paleozoic rocks, and sediments derived from those rocks is a source of high  $^{87}\text{Sr}/^{86}\text{Sr}$  in the groundwater.

Contours of  $^{87}\text{Sr}/^{86}\text{Sr}$  indicate that values of 0.7100 or greater are in a zone that corresponds to the hypothesized regional flow path (Fig. 7). Highest  $^{87}\text{Sr}/^{86}\text{Sr}$  values are at the upgradient end of the regional flow path, and the data indicate decreasing  $^{87}\text{Sr}/^{86}\text{Sr}$  values along the main flow path. Lower  $^{87}\text{Sr}/^{86}\text{Sr}$  values, consistent with water dominated by dissolution of Permian gypsum or anhydrite, are found north of the flow path at the southeastern edge of the Rustler Hills, which comprise Permian evaporites and carbonates. Lower  $^{87}\text{Sr}/^{86}\text{Sr}$  values also occur south of the flow path in low-TDS waters originating in the Wylie and Davis Mountains, which are composed of Permian carbonates and Eocene to Oligocene lavas and ash-flow tuffs, respectively. Based on this pattern, we initially hypothesized that samples along the regional flow path are a mixture of three end-members with no significant subsequent mineral-water reactions. End member A is high- $^{87}\text{Sr}/^{86}\text{Sr}$ , low-TDS,  $\text{Na}-\text{HCO}_3$  water originating in Wildhorse Flat at the upgradient end of the proposed regional flow system. End member B is low-TDS  $\text{Ca}-\text{Na}-\text{HCO}_3$  water from the Wylie and Davis Mountains with  $^{87}\text{Sr}/^{86}\text{Sr}$  values ranging from 0.7076–0.7082. End member C is higher TDS water from the Rustler Aquifer with  $^{87}\text{Sr}/^{86}\text{Sr}$  values similar to end member B and with a  $\text{Ca}-\text{SO}_4$  signature that indicates water chemistry dominated by anhydrite dissolution.

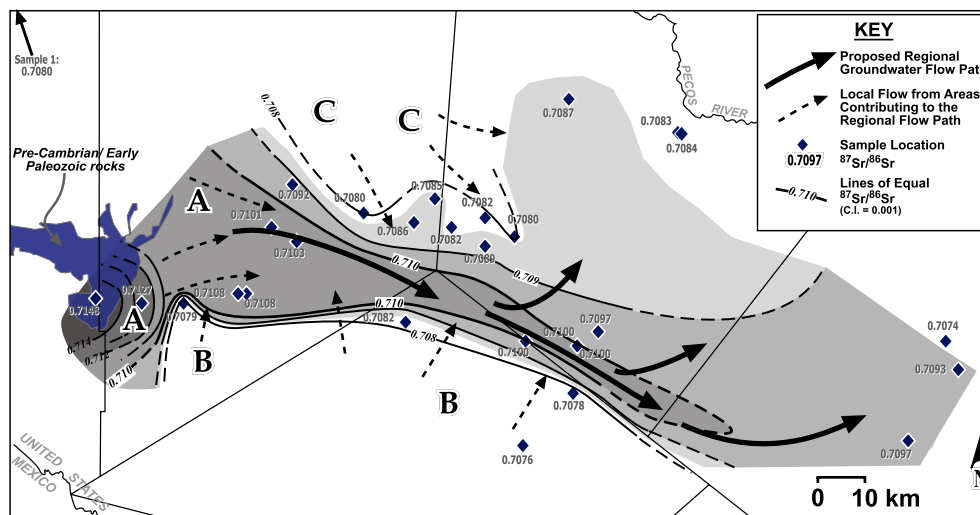


**Figure 7** Contours of  $^{87}\text{Sr}/^{86}\text{Sr}$  values from groundwater samples in relation to the hypothesized regional flow paths. The shaded areas represent  $^{87}\text{Sr}/^{86}\text{Sr}$  values that exceed 0.7084; darker shades represent higher  $^{87}\text{Sr}/^{86}\text{Sr}$  values. Areas A, B, and C are explained in the text.

## Models of chemical and isotopic evolution

Strontium concentrations, strontium isotope values, and mass-balance mixing models that test the three end-member mixing hypothesis are presented in Fig. 8a. All samples from locations along the regional flow path, except for sample 9, plot above the mixing lines, indicating that mixing of the three end-member solutions alone cannot account for the observed Sr concentrations and isotope values. This suggests the alternative hypothesis that the observed Sr isotope ratios along the regional flow path are produced by mixing of the three end members with some modification by subsequent mineral–water reactions.

A possible scenario supporting this hypothesis is that water from end member area A is dissolving strontium-bearing mineral phases in the alluvial fill of Wildhorse Flat, resulting in water chemistry similar to that observed in samples 5 and 6. Groundwater then flows out of Wildhorse Flat into the main regional flow system where it subsequently evolves through mixing with waters from end-member areas B and C. This scenario is tested with a two-step model.

the first step, mineral–water interactions in Wildhorse Flat are simulated using a conservative mineral dissolution model (based on Banner et al., 1989), represented by the dashed line on Fig. 8b. This model adds moles of Sr, with a specified  $^{87}\text{Sr}/^{86}\text{Sr}$  value, to a starting solution and calculates the changes in Sr concentration and isotope ratios as Sr is added. This model is based on Eq. (1):

$$([\text{Sr}_{(\text{target})}] \times ^{87}\text{Sr}/^{86}\text{Sr}_{(\text{target})}) = ([\text{Sr}_{(\text{start})}] \times ^{87}\text{Sr}/^{86}\text{Sr}_{(\text{start})}) + ([\text{Sr}_{(\text{min})}] \times ^{87}\text{Sr}/^{86}\text{Sr}_{(\text{min})}) \quad (1)$$

where  $[\text{Sr}_{(x)}]$  is the concentration of strontium in the target water sample, the starting water sample, and the amount added by dissolution of the mineral phase. Sample 3 is chosen as the starting solution. The dashed line on Fig. 8b represents addition of Sr from a mineral phase with  $^{87}\text{Sr}/^{86}\text{Sr} = 0.7105$ . Model results indicate that dissolution of  $3.1 \times 10^{-5}$  moles of Sr per liter at that ratio will reproduce the Sr concentration and isotope ratio of the target water composition (sample 6).

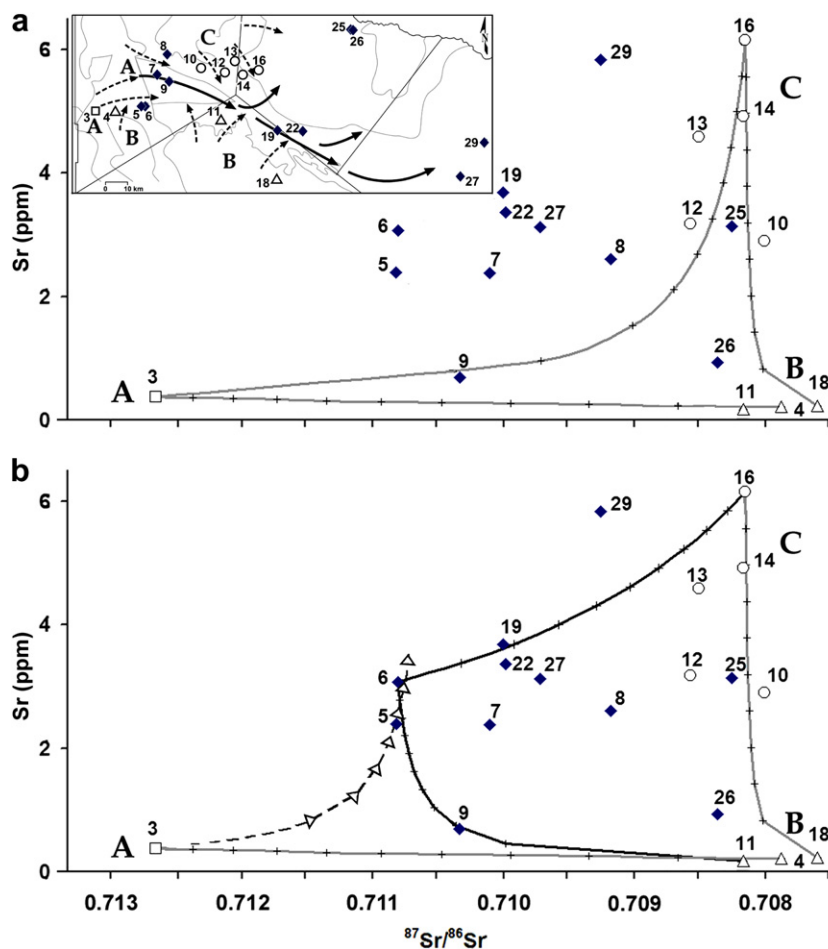


**Figure 8** Sr concentrations versus  $^{87}\text{Sr}/^{86}\text{Sr}$  with mixing and mineral dissolution models. The samples from end member areas A, B, and C, as identified on inset map, are represented by an open square, open triangles, and open circles, respectively. Other samples are represented by closed diamonds. (a) Solid lines indicate mass-balance mixing models with tick marks at 10% mixing increments. (b) Solid lines indicate mass-balance mixing models with tick marks at 10% mixing increments; the dashed line represents the mineral dissolution model. Arrowheads on dashed line indicate 0.005 mmol/L increments of Sr dissolved. *Inset map*: sample locations with the same symbols.

This model does not identify the specific mineral phase or phases which are dissolving. The major ion chemistry of samples 3, 5, and 6, as well as other samples taken from nearby wells (Fig. 9), indicates that, as water flows through the subsurface in Wildhorse Flat, Ca, Mg, Na,  $\text{SO}_4$ , and Cl concentrations are increasing,  $\text{HCO}_3$  concentrations are increasing slightly, and Si concentrations are decreasing. These data suggest that dissolution of halite and anhydrite, along with incongruent dissolution of dolomite (dolomite dissolution with calcite precipitation), are dominating the evolution of groundwater in Wildhorse Flat. This is consistent with the chemical evolution of groundwater in the main part of the regional flow system as described in Uliana and Sharp (2001). The inverse modeling subroutine in PHREEQC (Parkhurst, 1995; Parkhurst et al., 1980) was used to calculate possible mineral phase reactions that could account for the major ion chemistry of sample 6. Anhydrite, calcite, dolomite, halite, and  $\text{CO}_2(\text{g})$  were specified as mineral constraints, and sample 6 was specified as the target sample. PHREEQC model results (model 1 in Table 2) confirm that dissolution of anhydrite, dolomite, and halite, and precipitation of calcite, can produce water with chemistry similar to sample 6. Based on published data, Sr concentrations in these mineral phases range from 40–400 ppm for calcite, 20–200 ppm for dolomite, and 500–6300 ppm for anhydrite (Kinsman, 1969; Butler, 1973; Feng et al., 1997; Denison et al., 1994; Jacobson and Wasserburg, 2005). These concentration ranges were multiplied by the mole transfers for their respective mineral phases as calculated by the inverse model to determine the ranges of potential Sr contribution from the various mineral phases (Table 2).

Model results indicate that Sr contribution from dolomite dissolution is at least two orders of magnitude lower than the amount required to produce the Sr concentration observed in sample 6, suggesting that dolomite dissolution cannot contribute enough Sr to affect the isotope ratio. The Sr contribution required to produce sample 6 is, however, within the range of values calculated for anhydrite

dissolution (i.e.,  $2.7 \times 10^{-6}$ – $3.4 \times 10^{-5}$  mol). If it is assumed that anhydrite dissolution is controlling the Sr concentration in the groundwater in Wildhorse Flat, the dissolving anhydrite would require a Sr content of 5700 ppm (Table 2). This value is within the published range of values for anhydrite Sr content. The anhydrite Sr content and the conclusion that Sr isotope values in this regional flow system are controlled by anhydrite dissolution are consistent with the results of Jacobson and Wasserburg (2005) for the Madison aquifer of South Dakota.

The results of model 1 indicate a total mole transfer of approximately 0.01 mol/kg between the solution and the carbonate and sulfate mineral phases, or a log mineral–water ratio of  $-3.6$ . Quantitative modeling of the effects of mineral–water interactions on solution  $\delta^{18}\text{O}$  values for groundwater in carbonates (Banner et al., 1989) indicated that solution  $\delta^{18}\text{O}$  values are not affected until the log of the molar mineral–water ratio exceeds  $-2$ . Since the oxygen isotope fractionation factor for anhydrite is not significantly different from that for calcite (Zheng, 1999), the results of model 1 indicate that the extent of mineral–water reaction required to change the Sr isotope values to match the target solution would not affect the  $\delta^{18}\text{O}$  values in the samples and would not result in deviations of the data from the meteoric water line.

In the second model step, mixing of the groundwater leaving Wildhorse Flat and entering the main flow system is simulated using mass-balance mixing models, represented by the solid black lines on Fig. 8b. All samples located along the hypothesized regional flow path fall within those mixing curves. The only sample which does not fall within the mixing lines is sample 29, located at the eastern end of the study area. This sample plots above the mixing lines, suggesting that additional mineral phase dissolution could occur. The Sr concentrations and isotope ratios of sample 29 were simulated by the same strontium dissolution model with mineral phase mole transfers calculated by PHREEQC using samples 6, 19, and 27 as starting samples. Model results, labeled 2 through 4, are shown in Table 2.

The amount of Sr required to reproduce the Sr concentration in sample 29 is similar for each model. Models 2 and 3 require mineral phase  $^{87}\text{Sr}/^{86}\text{Sr}$  values that are consistent with the expected Sr isotope values for Permian and Cretaceous marine sediments. However, each model requires anhydrite with a Sr content greater than the published range of values (8000 ppm) and each also requires precipitation of halite, which is an unlikely possibility as halite saturation indices for all samples in the study area are  $-3$  or less. Model 4 does not require precipitation of halite; however, it does require a Sr content greater than published ranges (10,000 ppm) and mineral phase  $^{87}\text{Sr}/^{86}\text{Sr}$  values that are slightly higher than expected for Permian and Cretaceous marine sediments. A sample from end-member area B (sample 18) was also added as a PHREEQC constraint to models 2 through 4 to investigate possible mixing relationships. The PHREEQC inverse modeling routine, with an uncertainty of 0.05, did not produce any minimal models that included mixing (refer to Parkhurst, 1995, p. 31 for an explanation of the PHREEQC inverse model routine and a definition of ‘‘minimal models’’). Therefore, while the  $^{87}\text{Sr}/^{86}\text{Sr}$  value for sample 29 suggests that it is influenced by the regional flow system, the models devel-

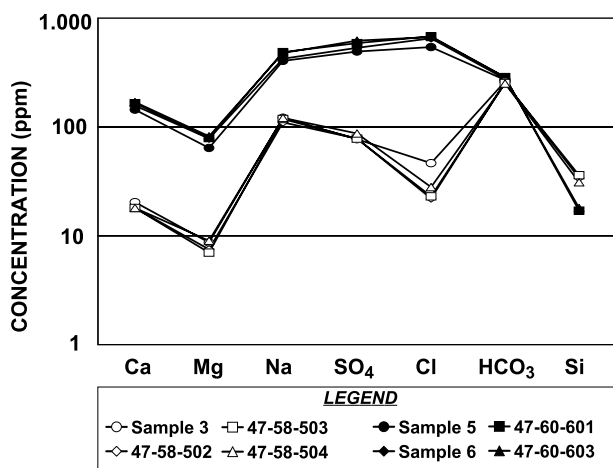


**Figure 9** Ion chemistry of samples 3, 5, and 6, with additional samples obtained from the Texas Water Development Board water well database. Samples with open symbols are from wells located within 5 km of sample 3; samples with closed symbols are located within 5 km of samples 5 and 6.

**Table 2** Mineral dissolution and PHREEQC inverse model results

1. Evolve sample 3 to sample 6				
(a) Add $3.1 \times 10^{-5}$ moles Sr per liter at $^{87}\text{Sr}/^{86}\text{Sr} = 0.7105$				
(b) Phase mole transfers		(c) Mole Transfer of Sr		(d) mineral [Sr]
		Low <sup>1</sup>	High <sup>2</sup>	
Dissolve anhydrite	0.0054	2.7E-06	3.4E-05	5,700
Precipitate calcite	-0.0049	-2.0E-07	-2.0E-06	
Dissolve dolomite	0.0025	5.0E-08	5.0E-07	
Dissolve halite	0.0153	-	-	
2. Evolve sample 6 to sample 29				
(a) Add $3.1 \times 10^{-5}$ moles Sr per liter at $^{87}\text{Sr}/^{86}\text{Sr} = 0.7076$				
(b) Phase mole transfers		(c) Mole Transfer of Sr		(d) mineral [Sr]
		Low <sup>1</sup>	High <sup>2</sup>	
Dissolve anhydrite	0.0039	2.0E-06	2.5E-05	8,000
Precipitate calcite	-0.0029	-1.2E-07	-1.2E-06	
Dissolve dolomite	0.0015	2.9E-08	2.9E-07	
Precipitate halite	-0.0039	-	-	
3. Evolve sample 19 to sample 29				
(a) Add $2.5 \times 10^{-5}$ moles Sr per liter at $^{87}\text{Sr}/^{86}\text{Sr} = 0.7080$				
(b) Phase mole transfers		(c) Mole Transfer of Sr		(d) mineral [Sr]
		Low <sup>1</sup>	High <sup>2</sup>	
Dissolve anhydrite	0.0031	1.5E-06	1.9E-05	8,000
Precipitate calcite	-0.0025	-9.9E-08	-9.9E-07	
Dissolve dolomite	0.0012	2.5E-08	2.5E-07	
Precipitate halite	-0.0030	-	-	
4. Evolve sample 27 to sample 29				
(a) Add $3.1 \times 10^{-5}$ moles Sr per liter at $^{87}\text{Sr}/^{86}\text{Sr} = 0.7089$				
(b) Phase mole transfers		(c) Mole transfer of Sr		(d) mineral [Sr]
		Low <sup>1</sup>	High <sup>2</sup>	
Dissolve anhydrite	0.0031	1.5E-06	1.9E-05	10,000
Precipitate calcite	-0.0039	-1.6E-07	-1.6E-06	
Dissolve dolomite	0.0020	3.9E-08	3.9E-07	
Dissolve halite	0.0031	-	-	

(a) moles of Sr required to produce the Sr concentration of the target solution from the starting solution; (b) mole transfers of the various phases calculated by the PHREEQC inverse modeling routine; (c) range of Sr contributions from the various phases based on the range of Sr concentrations in those minerals as described in the text; (d) calculated Sr content of anhydrite assuming that all of the Sr added to the target solution is from anhydrite dissolution. <sup>1</sup>Low range of Sr concentrations for anhydrite, calcite, and dolomite are 500, 40, and 20 ppm, respectively. <sup>2</sup>High range of Sr concentrations for anhydrite, calcite, and dolomite are 6300, 400, and 200 ppm, respectively.

oped here cannot fully explain the observed chemistry of this sample.

The relationship between  $^{87}\text{Sr}/^{86}\text{Sr}$  and  $\delta^{18}\text{O}$  provides an additional test of the regional flow hypothesis. A set of samples that represent points along the flow path (Fig. 10, inset) were selected. All of these samples have  $^{87}\text{Sr}/^{86}\text{Sr}$  values greater than expected for waters controlled by interactions with Permian and Cretaceous marine sediments ( $>0.7084$ ) and have  $\delta^{18}\text{O}$  values that are lower than the assumed value for local recharge ( $<-7.5\text{‰}$ ). A plot of  $\delta^{18}\text{O}$  versus  $^{87}\text{Sr}/^{86}\text{Sr}$  for these samples (Fig. 10) shows an overall trend of decreasing  $^{87}\text{Sr}/^{86}\text{Sr}$  along the flow path.  $\delta^{18}\text{O}$  values at the upgradient end of the flow path ( $-7.7\text{‰}$ ) are slightly lower than expected for local recharge.  $\delta^{18}\text{O}$  values decrease along the flow path to reach a low of  $-9.2\text{‰}$  in the Apache Mountains, then increase along the remainder of the path to a value at Comanche Springs in Fort Stockton near the expected range for local recharge ( $-7.5\text{‰}$ ). The trend between Van Horn and the Apache Mountains is interpreted

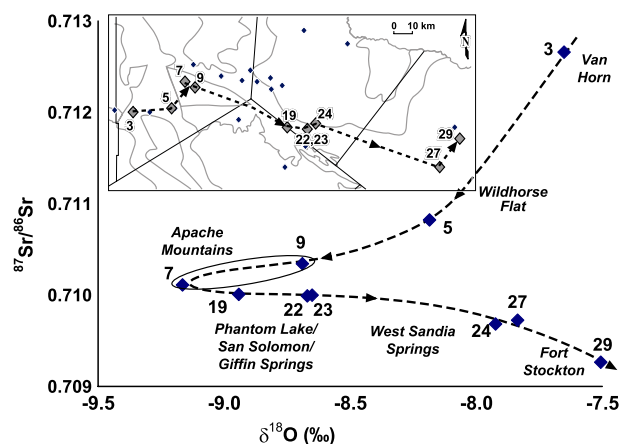


**Figure 10**  $^{87}\text{Sr}/^{86}\text{Sr}$  versus  $\delta^{18}\text{O}$ . The dashed line represents the order of the samples along the hypothesized gradient. *Inset map*: Sample locations.

as representing progressively older water along the flow path. The trend over the remainder of the flow path is interpreted as representing older recharge mixing with more recent recharge from the Davis Mountains. This trend is consistent with the trends in the geochemical evolution of water in the flow systems as described by Uliana and Sharp (2001), who identified older water from the regional system and from the Rustler Hills area mixing with more recent recharge at the springs north of the Davis Mountains.

## Conclusions

$\delta^{18}\text{O}$  and  $\delta\text{D}$  values for all groundwater samples from the Trans-Pecos regional study area plot on or close to the meteoric water line, indicating that the stable isotope values in the groundwater have not been significantly modified by extensive evaporation or mineral–water interactions.  $\delta^{18}\text{O}$  values from samples along the regional flow path are significantly lower than expected for recent meteoric recharge. These low values are interpreted as resulting from recharge to the regional groundwater system during the cooler and wetter climate of the late Pleistocene.

$^{87}\text{Sr}/^{86}\text{Sr}$  values and major ion chemistry in groundwater samples from the Davis Mountains and from groundwaters dominated by dissolution of Permian marine sedimentary rocks are consistent with expected values. Samples from the regional flow path have significantly higher  $^{87}\text{Sr}/^{86}\text{Sr}$  values than expected for waters dominated by dissolution of Permian and Cretaceous marine sedimentary rocks. These high values are consistent with interaction of groundwater with Precambrian and early Paleozoic rocks, at the upgradient end of the regional flow system.

The oxygen and strontium isotopes, and variations in the ion concentrations, suggest the presence of a three end-member fluid mixing system with modification by mineral dissolution. Mass balance fluid mixing models and mineral-reaction models indicate that high- $^{87}\text{Sr}/^{86}\text{Sr}$ , low-TDS,  $\text{Na}-\text{HCO}_3$  water from the upgradient end of the proposed flow system is dissolving anhydrite, dolomite, and halite while precipitating calcite as it flows through the alluvial fill of Wildhorse Flat. These models also indicate that the dissolution of anhydrite is controlling the Sr concentrations and isotope values of the groundwater. As water flows out of Wildhorse Flat into the main, fracture-controlled flow path, it is subject to mixing with low- $^{87}\text{Sr}/^{86}\text{Sr}$ , low-TDS,  $\text{Ca}-\text{Na}-\text{HCO}_3$  water from the Davis and Wylie Mountains, and low- $^{87}\text{Sr}/^{86}\text{Sr}$ , variable-TDS,  $\text{Ca}-\text{SO}_4$  water from the Rustler Formation. The geochemical reactions and mixing relationships are consistent with previous studies, and all support the hypothesis of a regional flow system in Trans-Pecos, Texas.

## Acknowledgements

This research was supported by grants from the Geological Society of America and the Jackson School of Geological Sciences at The University of Texas at Austin. The authors would like to thank Larry Mack, Libby Stern, and Phil Bennett for lending their analytical expertise. Early drafts of this manuscript benefited greatly from the review and cri-

tique of Patricia Dickerson and Alan Dutton. The authors would also like to thank the editors of *Journal of Hydrology* and the two anonymous reviewers for their helpful comments and suggestions.

## References

- Allison, G.B., 1982. The relationship between  $^{18}\text{O}$  and deuterium in water and in sand columns undergoing evaporation. *Journal of Hydrology* 76, 1–25.
- Anderson, R.S., 1993. A 35,000-year vegetation and climate history from Potato Lake, Mogollon Rim, Arizona. *Quaternary Research* 40, 233–252.
- Armstrong, S.C., Struchio, N.C., Hendry, M.J., 1998. Strontium isotopic evidence on the chemical evolution of pore waters in the Milk River aquifer, Alberta, Canada. *Applied Geochemistry* 13, 46–475.
- Ashworth, J.B., 1990. Evaluation of ground-water resources in parts of Loving, Pecos, Reeves, Ward, and Winkler Counties, Texas. Texas Water Development Board Report 317, 51 p.
- Babiker, M., Gudmundsson, A., 2004. The effects of dykes and faults on groundwater flow in an arid land; the Red Sea Hills, Sudan. *Journal of Hydrology* 297 (1–4), 256–273.
- Banner, J.L., Kaufman, J., 1994. The isotopic record of ocean chemistry and diagenesis preserved in non-luminescent brachiopods from Mississippian carbonate rocks, Illinois and Missouri. *Geological Society of America Bulletin* 106, 1074–1082.
- Banner, J.L., Wasserburg, G.J., Dobson, P.F., Carpenter, A.B., Moore, C.H., 1989. Isotopic and trace-element constraints on the origin and evolution of saline groundwaters from central Missouri. *Geochimica et Cosmochimica Acta* 53, 383–398.
- Banner, J.L., Musgrove, M.L., Capo, R.C., 1994. Tracing groundwater evolution in a limestone aquifer using Sr isotopes: effects of multiple sources of dissolved ions and mineral-solution reactions. *Geology* 22, 687–690.
- Barnes, V.E., 1976. Geologic atlas of Texas, Pecos Sheet: The University of Texas at Austin Bureau of Economic Geology, map with explanation.
- Barnes, V.E., 1979. Geologic atlas of Texas, Marfa Sheet: The University of Texas at Austin Bureau of Economic Geology, map with explanation.
- Barnes, V.E., 1995a. Geologic atlas of Texas, Fort Stockton Sheet: The University of Texas at Austin Bureau of Economic Geology, map with explanation.
- Barnes, V.E., 1995b. Geologic atlas of Texas, Van Horn-El Paso Sheet: The University of Texas at Austin Bureau of Economic Geology, map with explanation.
- Brookins, D.G., 1988. Seawater  $^{87}\text{Sr}/^{86}\text{Sr}$  for the Late Permian Delaware Basin evaporites; New Mexico, U.S.A. *Chemical Geology* 69, 209–214.
- Brune, G., 1981. Springs of Texas: Volume I. Branch-Smith, Inc., Fort Worth, 566 p.
- Burke, W.H., Dennison, R.E., Hetherington, E.A., Koepnick, R.B., Nelson, H.F., Otto, J.B., 1982. Variation of seawater  $^{87}\text{Sr}/^{86}\text{Sr}$  throughout Phanerozoic time. *Geology* 10, 516–519.
- Butler, G.P., 1973. Strontium geochemistry of modern and ancient calcium sulfate minerals. In: Purser, B.H. (Ed.), *The Persian Gulf: Holocene Carbonate Sedimentation and Diagenesis in a Shallow Epicontinental Sea*. Springer-Verlag, New York, pp. 423–452.
- Cameron, K.L., Parker, D.F., Sampson, D.E., 1996. Testing crustal melting models for the origin of flood rhyolites: a Nd-Pb-Sr isotopic study of the Tertiary Davis Mountains volcanic field, west Texas. *Journal of Geophysical Research* 101, 20,407–20,422.
- Clark, I.D., Fritz, Peter., 1997. *Environmental Isotopes in Hydrogeology*. Lewis Publishers, New York, 328 p.

- Coleman, M.L., Shepherd, T.J., Durham, J.J., Rouse, J.E., Moore, G.R., 1982. Reduction of water with zinc for hydrogen isotope analysis. *Analytical Chemistry* 54, 993–995.
- Coplen, T.B., Kendall, C., 2000. Stable hydrogen and oxygen isotope ratios for selected sites of the U.S. Geological Survey's NASQAN and Benchmark surface-water networks, U.S. Geological Survey Open-File Report 00-160, 409 p.
- Craig, H., 1961. Isotope variation in meteoric waters. *Science* 133, 1702–1703.
- Dansgaard, W., 1964. Stable isotopes in precipitation. *Tellus* 16, 436–468.
- Darling, B.K., 1997. Delineation of the ground-water flow systems of the Eagle Flat and Red Light Basins of Trans-Pecos Texas: Ph.D. dissertation, The University of Texas at Austin, 179 p.
- Denison, R.E., Koepnick, R.B., Burke, W.H., Hetherington, E.A., Fletcher, A., 1994. Construction of the Mississippian, Pennsylvanian and Permian seawater  $^{87}\text{Sr}/^{86}\text{Sr}$  curve. *Chemical Geology* 112, 145–167.
- Denison, R.E., Kirkland, D.W., Evans, R., 1998. Using strontium isotopes to determine the age and origin of gypsum and anhydrite beds. *Journal of Geology* 106, 1–17.
- Dutton, A.R., 1995. Groundwater isotopic evidence for paleorecharge in the U.S. High Plains aquifers. *Quaternary Research* 43, 221–231.
- Faure, G., 1986. *Principles of Isotope Geology*. Wiley, New York, 589 p.
- Feng, H.L., Meyers, W.J., Schoonen, M.A.A., 1997. Minor and trace element analyses on gypsum: an experimental study. *Chemical Geology* 142 (1-2), 1–10.
- Fontes, J.Ch., 1980. Environmental isotopes in groundwater hydrology. In: Fritz, P., Fontes, J.Ch. (Eds.), *Handbook of Environmental Isotope Geochemistry*. Elsevier, Amsterdam, pp. 411–440.
- Gates, J.S., White, D.E., Stanley, W.D., Ackerman, H.D., 1980. Availability of fresh and slightly saline ground water in the basins of westernmost Texas. Texas Department of Water Resources, Report #256, 108 p.
- Higgins, P., MacFadden, J., 2004. Amount Effect recorded in oxygen isotopes of Late Glacial horse (*Eqqus*) and bison (*Bison*) teeth from the Sonoran and Chihuahuan deserts, southwestern United States. *Palaeogeography, Palaeoclimatology, Palaeoecology* 206, 337–353.
- Hoyt, C.A., 2000. Grassland to desert: Holocene vegetation and climate change in the Northern Chihuahuan Desert: Ph.D. dissertation, The University of Texas at Austin.
- IAEA/WMO, 2001. Global Network of Isotopes in Precipitation. The GNIP Database, Station 7622500. Accessible at: <http://isohis.iaea.org>.
- Jacobson, A.D., Wasserburg, 2005. Anhydrite and the Sr isotope evolution of groundwater in a carbonate aquifer. *Chemical Geology* 214, 331–350.
- Kendall, C., Coplen, T.B., 1985. Multisample conversion of water to hydrogen by zinc for stable isotope determination. *Analytical Chemistry* 57, 1437–1440.
- Kinsman, D.J.J., 1969. Interpretation of  $\text{Sr}^{+2}$  concentrations in carbonate minerals and rocks. *Journal of Sedimentary Petrology* 39, 486–508.
- LaFave, J.L., Sharp, J.M., 1990. Origins of ground water discharging at the springs of Balmorhea. In: Kreitler, C.W., Sharp, J.M. (Eds.), *Hydrogeology of Trans-Pecos Texas*, 25. The University of Texas at Austin Bureau of Economic Geology Guidebook, pp. 91–100.
- Larkin, T.J., Bomar, G.W., 1983. Climatic Atlas of Texas. Texas Department of Water Resources Publication LP-192, 151 p.
- Mayer, J.M., Sharp Jr., J.M., 1998. Fracture control of regional ground-water flow in a carbonate aquifer in a semi-arid region. *Geological Society of America Bulletin* 110, 269–283.
- Mickler, P., Banner, J.L., Stern, L.A., Asmerom, Y., Edwards, R.L., Ito, E., 2004. Stable isotope variations in modern tropical speleothems: Evaluating equilibrium versus kinetic isotope effects. *Geochimica et Cosmochimica Acta*. 68, 4381–4393.
- Musgrove, M., Banner, J.L., 1993. Regional groundwater mixing and the origin of saline fluids: Midcontinent, United States. *Science* 259, 1877–1882.
- Neilson, P.D., Sharp, J.M., 1985. Tectonic controls on the hydrogeology of the Salt Basin, Trans-Pecos Texas. In: Dickerson, P.W., Muehlberger, W.R. (Eds.), *Structure and Tectonics of Trans-Pecos Texas*, 85-81. West Texas Geological Society Publication, pp. 231–234.
- Parkhurst, D.L., 1995. User's guide to PHREEQC – a computer program for speciation, reaction-path, advective-transport, and inverse geochemical calculations: U.S. Geological Survey Water Resources Investigations Report 95-4227, 143 p.
- Parkhurst, D.L., Thorstenson, D.C., Plummer, N.L., 1980. PHREEQC – a computer program for geochemical calculation: U.S. Geological Survey Water Resource Investigation Report 80-96.
- Rosanski, K., Araguas-araguas, L., Gonfiantini, R., 1993. Isotopic patterns in modern global precipitation. In: Swart, P.K., Lobmann, K.C., McKenzie, J., Savin, S. (Eds.), *Climate Change in Continental Isotopic Records: American Geophysical Union Geophysical Monograph*, 78, 1–36.
- Scanlon, B.R., Goldsmith, R.S., Langford, R.P., 2000. Relationship between arid geomorphic settings and unsaturated zone flow: case study, Chihuahuan Desert, Texas: The University of Texas at Austin Bureau of Economic Geology Report of Investigations No. 261, 133 p.
- Schuster, S.K., 1996. Water resource and planning assessment in San Solomon Springs and associated spring systems surrounding Balmorhea, Texas: M. S. report, The University of Texas at Austin, 102 p.
- Sharp, J.M. Jr., 1989. Regional ground-water systems in northern Trans-Pecos Texas. In: Dickerson, P.W., Muehlberger, W.R. (Eds.), *Structure and Stratigraphy of Trans-Pecos Texas*. American Geophysical Union Field Trip Guidebook T317, 123–130.
- Sharp, J.M. Jr., Halihan, T., Uliana, M.M., Tsofiias, G.P., Landrum, M.T., Marrett, R., 2000. Predicting fractured rock hydrogeological parameters from field and laboratory data. In: Sililo, O. (Ed.), *Groundwater: Past Achievements and Future Challenges*, Proceedings of the 30th Congress, International Association of Hydrogeologists, Cape Town, South Africa, p. 319–324.
- Stute, M., Schlosser, P., Clark, J.F., Broecker, W.S., 1992. Paleotemperatures in the southwestern United States derived from noble gas measurements in groundwater. *Science* 256, 1000–1003.
- Stute, M., Clark, J.F., Schlosser, P., Broecker, W.S., 1995. A 30,000 year continental paleotemperature record derived from noble gases dissolved in groundwater from the San Juan Basin, New Mexico. *Quaternary Research* 43, 209–220.
- Toomey III, R.S., Blum, M.D., Salvatore Jr., V., 1993. Late Quaternary climates and environments of the Edwards Plateau, Texas. *Global and Planetary Change* 7 (4), 299–320.
- Uliana, M.M., 2000. Delineation of regional groundwater flow paths and their relation to structural features in the Salt and Toyah Basins, Trans-Pecos Texas: Ph.D. Dissertation, The University of Texas at Austin, 215 p.
- Uliana, M.M., Sharp Jr., J.M., 2001. Tracing regional flow paths to major springs in Trans-Pecos Texas using geochemical data and geochemical models. *Chemical Geology* 179, 53–72.
- Van der Straaten, C.M., Mook, W.G., 1983. Stable isotope composition of precipitation and climate variability. In: *Paleoclimates and Paleowaters: a Collection of Environmental Isotope Studies* STI/PUB/621. International Atomic Energy Agency, Vienna, pp. 53–64.
- Wood, J., 1965. Geology of the Apache Mountains, Trans-Pecos Texas: Ph. D. dissertation, The University of Texas at Austin, 241 p.
- Zheng, Y.-F., 1999. Oxygen isotope fractionation in carbonate and sulfate minerals. *Geochemical Journal* 33, 109–126.